Thickness of the Macula, Retinal Nerve Fiber Layer, and Ganglion Cell-inner Plexiform Layer in the Macular Hole: The Repeatability Study of Spectral-domain Optical Coherence Tomography

Woo Hyuk Lee, Young Joon Jo, Jung Yeul Kim

Department of Ophthalmology, Chungnam National University College of Medicine, Daejeon, Korea

Purpose: We measured the thicknesses of the ganglion cell and inner plexiform layer (GCIPL), the macula, and the retinal nerve fiber layer (RNFL) using spectral-domain optical coherence tomography in patients with idiopathic macula holes to analyze the repeatability of these measurements and compare them with those of the fellow eye.

Methods: We evaluated 85 patients who visited our retinal clinic. The patients were divided into two groups according to their macular hole size: group A had a size of <400 μm, while group B had a size of ≥400 μm. Repeatability was determined by comparing the thicknesses of the GCIPL, macula, and RNFL with those of the normal fellow eye.

Results: The average central macular thickness in patients with macular holes was significantly thicker than that in the normal fellow eye (343.8 ± 78.6 vs. 252.6 ± 62.3 μm, *p* < 0.001). The average thickness of the GCIPL in patients with macular holes was significantly thinner than that in the normal fellow eye (56.1 ± 23.4 vs. 77.1 ± 12.8 μm, *p* < 0.001). There was no significant difference in the average RNFL thickness between eyes with macular holes and fellow eyes (92.4 ± 10.0 vs. 95.5 ± 10.7 μm, *p* = 0.070). There were also no significant differences in the thicknesses of the GCIPL and RNFL among the two groups (*p* = 0.786 and *p* = 0.516). The intraclass correlation coefficients for the macula and RNFL were 0.994 and 0.974, respectively, in patients with macular holes, while that for the GCIPL was 0.700.

Conclusions: Macular contour change with macular hole results in low repeatability and a tendency of thinner measurement regarding GCIPL thickness determined via spectral-domain optical coherence tomography. The impact of changes in the macular shape caused by macular holes should be taken into consideration when measuring the GCIPL thickness in patients with various eye diseases such as glaucoma and in those with neuro-ophthalmic disorders.

Key Words: Macular holes, Repeatability, Retina, Spectral-domain optical coherence tomography

Macular holes, which are characterized by defects of the neurosensory retina and cystic changes in the macula, cause central visual disturbances [1]. Knapp [2] reported the first macular hole in 1869. More than 100 years later,

Gass [3] revealed that the cause of idiopathic macular holes is vitreomacular traction on the fovea in a tangential direction. Gaudric et al. [4] and Hee et al. [5] proposed the use of vitrectomy, which removes vitreomacular traction, as a successful treatment of macular holes.

Optical coherence tomography (OCT) is widely used to study macular disease because it displays the cross-sectional image of the retina at a high resolution and enables the quantitative evaluation of macular thickness. OCT recently evolved from the time domain to the spectral domain. Spectral-domain OCT (SD-OCT) results in images using Fourier transformation after the spectrum of the light through the interferometer is accepted by the spectrometer. This procedure can obtain more images in a shorter time as compared with time-domain OCT. In addition, with advanced image processing techniques, accurate analysis has been made possible by autosegmentation of each layer of the macula. According to the results of some investigations completed using autosegmentation, macular hole geometry and the extent of ellipsoid zone band defects are associated with postoperative visual acuity [6,7].

SD-OCT exhibits high repeatability and reproducibility in measuring the thickness of macular and peripapillary retinal nerve fiber layers (RNFLs) [8]. Quantitative measurement of the macular ganglion cell and inner plexiform layer (GCIPL) was recently made possible. The measurement of GCIPL autosegmentation is broadly used in various fields of ophthalmology. Mwanza et al. [9] and Mwanza et al. [10] found that the thickness of the GCIPL is useful for the evaluation of structural changes in the retina and provides critical information for the early diagnosis of glaucoma. In addition, Moon et al. [11] evaluated changes in the thickness of the GCIPL caused by various types of brain lesion in patients with visual impairment.

Mwanza et al. [10] and Francoz et al. [12] reported that automated measurement of the thickness of the GCIPL in normal and glaucomatous eyes exhibits a high level of repeatability; thus, the thickness of the GCIPL is useful for examining the progress of glaucoma. Furthermore, retinal changes can affect measurement repeatability; in particular, the thickness of the GCIPL as measured through the segmentations of the retina may be measured inaccurately. Some studies have shown that autosegmented measurements exhibit a high tendency to be erroneous in nonhealthy patients [6,7,13].

However, to our knowledge, no studies to date have examined the measurement repeatability of the GCIPL thickness in eyes with macular hole. Since macular hole shows structural abnormality only in the macula, it is thought to be adequate for studies on the effects of macular disease on GCIPL measurement. We assumed that GCIPL measurement would be different according to macular defect by hole size.

Therefore, using SD-OCT, we evaluated the measurement repeatability of the central macular thickness, peripapillary RNFL thickness, and GCIPL thickness in patients with idiopathic full-thickness macular holes. We compared these findings with those of normal eyes.

Materials and Methods

This prospective cohort study was approved by the institutional review board of Chungnam National University Hospital. The procedures used adhered to the tenets of the Declaration of Helsinki. The institutional review board of Chungnam National University Hospital also approved the prospective collection of data from the medical charts of patients with and without retinal diseases (2012-05-007). Prior to macular hole surgery, written informed consent was obtained not only for the surgery but also for the use of patients' data for future research studies.

Materials

The present study was carried out from June 2012 to October 2014. Patients who visited the retina clinic of Chungnam National University Hospital and who were diagnosed with unilateral idiopathic macular holes without participating ophthalmic history were included in this study. A detailed medical history as well as uncorrected visual acuity, best-corrected visual acuity, intraocular pressure using noncontact tonometry, funduscopy, fundus photography, and OCT findings were obtained from all of the patients (85 patients). Patients with axial lengths shorter than 23.60 mm and longer than 25.55 mm were excluded because these patients require the adjustment of measurements by SD-OCT [14]. Patients with a history of intraocular surgery, ocular trauma, diagnosis of other ophthalmic diseases in addition to macular holes (including retinal disease, glaucoma, and optic nerve disease), and those with OCT signal strength under 5 were excluded from this study [15].

OCT measurement

A macular cube 512 × 128 combination scan mode and an optic disc cube 200 × 200 scan mode were performed by an experienced examiner using SD-OCT (Cirrus HD-OCT; Carl Zeiss Meditec, Jena, Germany). Full-thickness and GCIPL were analyzed in the macular cube scans, while RNFL was analyzed in the optic disk cube scans. The measurement was repeated twice in five-minute intervals to examine the measurement repeatability. The macular cube 512 × 128 combination scan mode was analyzed after dividing it into a central circle, inner ring, and outer ring with diameters of 1, 3, and 6 mm, respectively, based on the center of the macula using a retinal map automated analysis system from the Cirrus HD-OCT software ver. 6.0.1. The scan was divided into the nine Early Treatment Diabetic Retinopathy Study subfields—specifically, the central macular subfield and the inner and outer superior, temporal, inferior, and nasal subfields (Fig. 1A) [16]. The RNFL was analyzed with respect to its average thickness and four areas obtained from the optic disc cube 200 × 200 scan mode (i.e., superior, temporal, inferior, nasal) (Fig. 1B).

The thickness of the GCIPL was measured using a ganglion cell analysis algorithm, which is a software system within the Cirrus HD-OCT ver. 6.0.1. Based on the three-dimensional information obtained from the macular cube scan, the thickness of the GCIPL was measured by detecting the boundaries of the outer boundary of the nerve fiber layer and the outer boundary of the inner plexiform layer (Fig. 1C, 2A, 2B). All measurements were determined automatically on a pixel-by-pixel basis for all of the SD-OCT images using an intraretinal layer automated segmentation method. Focusing on the fovea and after excluding internal ovals with a horizontal diameter of 1.2 mm and a vertical diameter of 1.0 mm, the average, minimum value, and six sectors (i.e., the superior, superotemporal, superonasal, inferior, inferonasal, and inferotemporal areas) were measured in the annulus with a horizontal diameter of 4.8 mm and a vertical diameter of 4.0 mm (Fig. 1C).

Each patient's affected eye was compared with their opposite normal eye. The affected eyes were divided into two groups according to the size of the macular hole. The areas with macular hole measuring <400 and ≥400 μm were classified into groups A and B, respectively, to analyze the influence of hole size on measurement. The size of the macular hole was defined as the base diameter from the retinal pigment epithelium, and the measurement was performed on both vertical and horizontal tomography, crossing the center of the macular hole on SD-OCT. The average measurements of the maximum horizontal and vertical diameters were used for analysis.
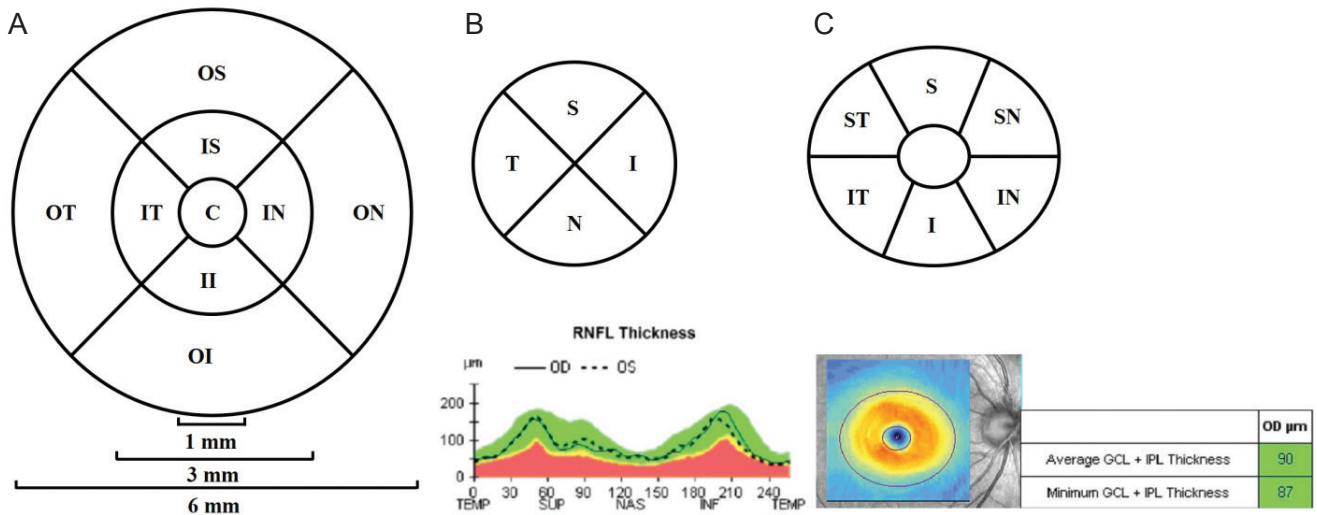
Fig. 1. Macular and optic disc analysis of the right eye. (A) A macular cube 512 × 128 combination scan mode, (B) an optic disc cube 200 × 200 scan mode, and (C) ganglion cell and inner plexiform layer analysis. OS = outer superior; OT = outer temporal; OI = outer inferior = ON = outer nasal; IS = inner superior; IT = inner temporal; II = inner inferior; IN = inner nasal; C = central; S = superior; T = temporal; I = inferior; N = nasal; RNFL = retinal nerve fiber layer; TEMP = temporal; SUP = superior; NAS = nasal; INF = inferior; ST = superotemporal; IT = inferotemporal; IN = inferonasal; SN = superonasal; GCL = ganglion cell layer; IPL = inner plexiform layer.

Statistical analysis

Analyses were performed with the PASW Statistics ver. 18.0 (SPSS Inc., Chicago, IL, USA). When comparing the affected eye and the normal fellow eye, Student's t-tests were used. In the comparison between groups A and B, Pearson's chi-squared test and Student's t-test were used. We employed the average measurement in the comparison. The intraclass correlation coefficient (ICC), coefficient of variation (COV), and test-retest variability (TRV) were calculated to determine the repeatability of consecutively measured thicknesses of the central macula, RNFL, and GCIPL. ICC is the correlation between two variables measured at different time points (t) with values ranging from 0 to 1. As the ICC value approaches 1, the repeatability of the measurement increases proportionally [17]. COV is the ratio of the standard deviation and the mean expressed as a percentage; the closer the value is to 0, the higher the repeatability is. TRV (μm), as indicated by the coefficient of repeatability, was calculated by multiplying the standard deviation of the difference between the measurements by 2. High repeatability was indicated by the existence of TRV values close to 0. The agreement between the two measurements was assessed using Bland-Altman plots, and p-values of <0.05 were deemed to indicate statistical significance [18].

Results

This study included 85 patients (29 males and 53 females). Groups A and B included 25 eyes and 57 eyes, respectively. There were no significant differences in terms of age, sex, laterality, best-corrected visual acuity, intraocular pressure, or refractive power among the two groups (Table 1).

OCT measurement with automated analysis

The thickness of the central macula, average thickness of the RNFL, and average thickness of the GCIPL among all patients were 252.6 ± 62.3, 92.4 ± 10.0, and 77.1 ± 12.8 μm, respectively, in normal fellow eyes and 343.8 ± 78.6, 95.5 ± 10.7, and 56.1 ± 23.4 μm, respectively, in eyes with macular holes. The thickness of the central macula was significantly thicker in affected eyes than in normal eyes ($p < 0.001$), while the thickness of the average GCLIPL was thinner in affected eyes than in normal eyes; it was also low in each sector ($p < 0.001$). There was no significant difference in the thickness of the RNFL ($p = 0.070$) (Table 2).

The analysis according to macular hole size showed that the average thicknesses of the central macula, RNFL, and GCIPL were 323.3 ± 47.1, 94.8 ± 12.1, and 53.7 ± 22.5 μm, respectively, in group A and 352.2 ± 83.6, 95.8 ± 10.5, and
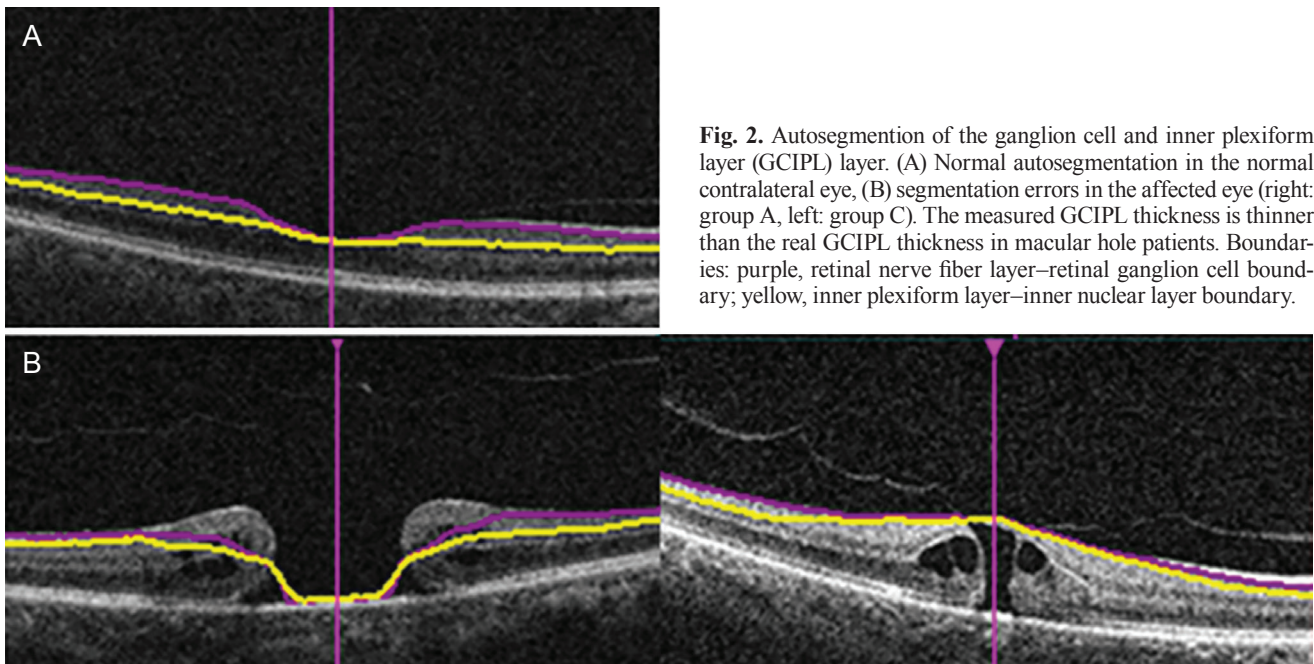
Fig. 2. Autosegmention of the ganglion cell and inner plexiform layer (GCIPL) layer. (A) Normal autosegmentation in the normal contralateral eye, (B) segmentation errors in the affected eye (right: group A, left: group C). The measured GCIPL thickness is thinner than the real GCIPL thickness in macular hole patients. Boundaries: purple, retinal nerve fiber layer–retinal ganglion cell boundary; yellow, inner plexiform layer–inner nuclear layer boundary.

Table 1. Patient demographics

	Total MH eyes (n = 85)	Group A (n = 25)	Group B (n = 57)	p-value[*]
Central macular thickness (µm)	343.4 ± 78.6	323.3 ± 47.1	352.2 ± 83.6	0.101
Age (yr)	68.3 ± 8.9	67.1 ± 9.1	68.6 ± 8.8	0.575
Sex (male : female)	29 : 53	8 : 17	21 : 36	0.757[†]
Laterality (OD : OS)	39 : 43	13 : 12	26 : 31	0.439[†]
BCVA (logMAR)	0.64 ± 0.11	0.72 ± 0.10	0.61 ± 0.10	<0.001
Intraocular pressure	14.5 ± 3.3	14.5 ± 2.9	14.6 ± 3.4	0.915
Axial length (mm)	24.42 ± 1.50	24.30 ± 1.59	24.44 ± 1.35	0.772
Refractive error (SE, diopters)	-0.01 ± 1.20	0.16 ± 1.10	-0.09 ± 1.20	0.483
MH size (µm)	570.7 ± 220.5	232.5 ± 106.2	804.7 ± 199.2	<0.001

MH = macular hole; OD = right eye; OS = left eye; BCVA: best-corrected visual acuity; logMAR = logarithm of the minimum angle of resolution; SE = spherical equivalent.
[*]Student's t-test, if not indicated; [†]Pearson's chi-squared test.

Table 2. Comparison of measurement values between eyes with macular holes and fellow eyes

		Fellow eye	Macular hole	p-value[*]
Macular thickness (µm)	Central	252.6 ± 62.3	343.8 ± 78.6	<0.001
	Inner superior	318.3 ± 34.1	345.1 ± 35.5	<0.001
	Inner temporal	313.0 ± 47.3	336.1 ± 35.2	<0.001
	Inner inferior	316.6 ± 38.1	343.3 ± 36.5	<0.001
	Inner nasal	320.1 ± 34.7	361.0 ± 44.0	<0.001
	Outer superior	278.6 ± 24.3	282.3 ± 25.6	0.791
	Outer temporal	270.5 ± 47.9	270.5 ± 31.3	0.950
	Outer inferior	264.7 ± 22.1	266.8 ± 26.0	0.857
	Outer nasal	296.1 ± 18.1	299.5 ± 29.0	0.527
RNFL thickness (µm)	Average	92.4 ± 10.0	95.5 ± 10.7	0.070
	Superior	115.3 ± 23.8	123.5 ± 37.5	0.041
	Temporal	70.5 ± 14.0	71.6 ± 14.8	0.582
	Inferior	119.7 ± 21.5	111.0 ± 37.4	0.154
	Nasal	68.5 ± 11.5	70.9 ± 15.6	0.415
GCIPL thickness (µm)	Average	77.1 ± 12.8	56.1 ± 23.4	<0.001
	Minimum	68.8 ± 19.4	35.8 ± 22.9	<0.001
	Superior	78.2 ± 13.2	58.5 ± 26.6	<0.001
	Superotemporal	78.3 ± 14.8	64.0 ± 25.2	<0.001
	Inferotemporal	79.1 ± 17.2	62.0 ± 25.1	<0.001
	Inferior	74.2 ± 18.2	49.5 ± 25.8	<0.001
	Inferonasal	76.8 ± 14.8	53.8 ± 26.0	<0.001
	Superonasal	79.5 ± 15.9	58.0 ± 27.5	<0.001

Values are presented as mean ± standard deviation.
RNFL = retinal nerve fiber layer; GCIPL = ganglion cell and inner plexiform layer.
[*]Student's t-test.

58.3 ± 23.3 μm, respectively, in group B. The thickness of the central macula, RNFL, and GCIPL were not significantly different among the two groups (Table 1, 3).

Measurement repeatability

The ICCs of the thicknesses of the central macula, RNFL, and GCIPL for healthy fellow eyes were 0.995, 0.966, and 0.998, respectively, whereas those for affected eyes were 0.994, 0.974, and 0.700. Both eye types exhibited an ICC of ≥0.950 for the central macula and RNFL, and they showed similar results to the measurements of each area of the central macula and RNFL. The ICC for the GCIPL of the affected eye was 0.700, which was lower than that for the RNFL and central macula; it was also low in each sector. The other markers of repeatability (i.e., COV

and TRV) yielded similar results (Table 4, 5). We assessed the same data using Bland-Altman plots (Fig. 3A-3C).

Discussion

The vitreoretinal interface is a complex structure of connective tissue that connects the vitreous cortex and inner retina. The posterior vitreous contains a high concentration of collagen fibers; laminin, fibronectin, and chondroitin are attached to the surface of the limiting membrane of the retina [19]. The close relationship between the vitreous cortex and the retina can lead to various vitreoretinal interface disorders, including idiopathic macular holes. Gass [3] reported the mechanism of macular holes as involving tangential traction around the fovea. Studies using OCT have

Table 3. Comparison of measurement values among the two groups

		Group A	Group B	p-value[*]
Macular thickness (μm)	Central	323.3 ± 47.1	352.2 ± 83.6	0.101
	Inner superior	326.5 ± 14.2	354.3 ± 36.7	<0.001
	Inner temporal	314.3 ± 13.8	341.2 ± 36.5	<0.001
	Inner inferior	321.1 ± 13.4	348.9 ± 37.9	<0.001
	Inner nasal	329.4 ± 18.3	369.0 ± 44.8	<0.001
	Outer superior	279.1 ± 12.3	279.9 ± 24.5	0.614
	Outer temporal	261.8 ± 8.3	263.1 ± 20.8	0.014
	Outer inferior	267.2 ± 8.5	266.6 ± 28.7	0.894
	Outer nasal	298.2 ± 13.9	298.6 ± 24.8	0.938
RNFL thickness (μm)	Average	94.8 ± 12.1	95.8 ± 10.5	0.786
	Superior	120.5 ± 23.1	123.4 ± 41.9	0.734
	Temporal	69.8 ± 16.7	73.5 ± 14.2	0.469
	Inferior	121.1 ± 16.4	108.8 ± 40.6	0.087
	Nasal	67.2 ± 13.6	71.8 ± 16.1	0.300
GCIPL thickness (μm)	Average	53.7 ± 22.5	58.3 ± 23.3	0.516
	Minimum	34.1 ± 25.4	36.4 ± 22.2	0.767
	Superior	52.8 ± 25.2	59.8 ± 26.8	0.382
	Superotemporal	56.0 ± 22.8	65.8 ± 25.3	0.185
	Inferotemporal	55.7 ± 24.9	63.4 ± 24.9	0.307
	Inferior	47.8 ± 23.4	49.7 ± 26.1	0.799
	Inferonasal	56.1 ± 22.6	52.9 ± 26.6	0.661
	Superonasal	53.7 ± 23.0	58.1 ± 28.6	0.559

Values are presented as mean ± standard deviation.
RNFL = retinal nerve fiber layer; GCIPL = ganglion cell and inner plexiform layer.
[*]Student's *t*-test.

Table 4. Comparison of measurement values in fellow eye

		First measured value (μm)	Second measured value (μm)	ICC	COV (%)	TRV (μm)
Macular thickness (μm)	Central	251.1 ± 33.8	251.7 ± 31.4	0.995	1.2	2.4
	Inner superior	319.5 ± 23.3	320.9 ± 23.7	0.994	0.8	2.1
	Inner temporal	312.4 ± 31.1	314.2 ± 23.3	0.956	1.0	1.9
	Inner inferior	313.6 ± 31.6	317.5 ± 25.3	0.922	1.0	2.9
	Inner nasal	319.4 ± 28.6	321.5 ± 25.6	0.981	0.8	2.7
	Outer superior	279.0 ± 21.0	276.5 ± 19.8	0.970	0.8	2.8
	Outer temporal	270.0 ± 23.1	271.9 ± 22.0	0.962	0.9	1.7
	Outer inferior	263.6 ± 18.5	265.3 ± 17.4	0.996	0.6	1.7
	Outer nasal	295.4 ± 18.6	296.3 ± 22.3	0.968	0.7	1.8
RNFL thickness (μm)	Average	94.1 ± 11.4	93.1 ± 10.0	0.966	1.2	0.9
	Superior	110.8 ± 19.5	105.6 ± 17.5	0.883	1.6	1.6
	Temporal	70.2 ± 13.0	69.3 ± 12.6	0.982	1.8	1.2
	Inferior	118.5 ± 19.5	119.2 ± 15.5	0.845	1.6	2.1
	Nasal	68.3 ± 15.9	68.5 ± 12.1	0.978	2.1	1.4
GCIPL thickness (μm)	Average	77.5 ± 8.1	77.0 ± 7.9	0.998	1.9	0.7
	Minimum	68.9 ± 9.8	69.0 ± 9.3	0.991	2.6	1.3
	Superior	79.0 ± 7.3	78.9 ± 8.3	0.981	2.0	1.6
	Superotemporal	78.5 ± 7.3	78.3 ± 7.8	0.996	1.8	0.8
	Inferotemporal	78.9 ± 11.5	79.0 ± 11.1	0.998	2.0	0.7
	Inferior	73.6 ± 7.8	74.0 ± 7.0	0.984	2.1	1.5
	Inferonasal	76.0 ± 8.7	76.7 ± 7.3	0.985	2.1	1.8
	Superonasal	79.6 ± 8.7	79.7 ± 9.2	0.991	2.2	1.2

Values are presented as mean ± standard deviation.
ICC = intraclass correlation coefficient; COV = coefficient of variation; TRV = test-retest variability; RNFL = retinal nerve fiber layer; GCIPL = ganglion cell and inner plexiform layer.

revealed that foveal cysts are created in the sensory retina by vitreous traction and develop into full-thickness macular holes as the internal and external walls are disrupted [3,20]. de Sisternes et al. [6] stated that the extent of ellipsoid zone band defects in the foveal and parafoveal regions was a good predictor of postoperative visual acuity recovery. Xu et al. [7] reported that macular hole geometry was related to pre- and postoperative visual acuity.

Measurements of the thickness of the macula and RNFL using SD-OCT in healthy eyes and glaucoma patients exhibit high levels of repeatability and reproducibility [21,22]. Pinilla et al. [23], who included normal fellow eyes in their study, reported that both time-domain OCT and SD-OCT showed highly reliable repeatability in the measurement of macular thickness.

Many studies on the thickness of the GCIPL are current-

ly ongoing in various ophthalmic fields. Park et al. [24] stated that the GCIPL of amblyopic eyes is thinner than that of normal eyes, while Kim et al. [25] highlighted an increased thickness of the GCIPL in patients with nonproliferative diabetic retinopathy after panretinal photocoagulation. In addition, some studies have reported a high reproducibility of GCIPL measurements using SD-OCT in patients with glaucoma [24,26]. Conversely, other studies have shown that autosegmented measurements demonstrate a high tendency to be erroneous in nonhealthy patients. Lee et al. [13] reported that macular contour change with epiretinal membrane results in low repeatability and a tendency to measure thinner GCIPL values using SD-OCT. Xu et al. [7] stated that errors in segmentation occurred predominantly at the edge of the macular hole boundary, where there was greater irregularity of the shape of the

Table 5. Comparison of measurement values in patients with macular holes

		First measured value (µm)	Second measured value (µm)	ICC	COV (%)	TRV (µm)
Macular thickness (µm)	Central	348.2 ± 125.5	345.8 ± 119.3	0.994	3.7	9.4
	Inner superior	348.5 ± 36.5	347.5 ± 34.7	0.982	10.9	7.7
	Inner temporal	340.3 ± 41.6	334.1 ± 36.0	0.883	12.7	25.5
	Inner inferior	343.4 ± 41.5	346.8 ± 40.2	0.898	13.3	22.9
	Inner nasal	360.7 ± 44.7	362.9 ± 45.7	0.998	14.1	2.0
	Outer superior	280.5 ± 21.4	280.9 ± 20.8	0.998	7.1	2.0
	Outer temporal	272.1 ± 22.8	270.8 ± 22.2	0.994	8.1	2.3
	Outer inferior	265.3 ± 24.8	265.7 ± 24.9	0.998	6.5	1.4
	Outer nasal	293.7 ± 19.2	292.5 ± 20.1	0.997	7.3	1.6
RNFL thickness (µm)	Average	95.7 ± 10.6	96.5 ± 11.5	0.974	3.0	0.9
	Superior	121.6 ± 16.4	123.6 ± 18.5	0.936	5.2	1.8
	Temporal	72.5 ± 12.9	73.1 ± 11.5	0.997	7.4	0.9
	Inferior	110.1 ± 19.6	115.1 ± 16.9	0.994	4.8	1.4
	Nasal	70.2 ± 15.1	71.6 ± 13.7	0.962	6.0	2.2
GCIPL thickness (µm)	Average	52.9 ± 20.4	58.6 ± 18.0	0.700	34.5	14.1
	Minimum	33.8 ± 24.0	38.6 ± 22.5	0.776	45.9	15.5
	Superior	49.5 ± 24.9	57.6 ± 21.3	0.657	36.4	13.4
	Superotemporal	55.0 ± 23.1	65.9 ± 18.9	0.801	32.0	13.8
	Inferotemporal	60.3 ± 23.0	61.1 ± 18.0	0.654	29.6	18.1
	Inferior	46.1 ± 22.8	49.9 ± 20.1	0.770	40.8	14.5
	Inferonasal	48.0 ± 22.8	53.7 ± 21.2	0.716	24.3	14.5
	Superonasal	54.1 ± 26.6	58.8 ± 24.8	0.724	33.0	18.1

Values are presented as mean ± standard deviation.
ICC = intraclass correlation coefficient; COV = coefficient of variation; TRV = test-retest variability; RNFL = retinal nerve fiber layer; GCIPL = ganglion cell and inner plexiform layer.

segmentation result. However, few studies have evaluated the repeatability of measurement of the GCIPL thickness according to macular defect in patients with retinal disease.

The thicknesses of the GCIPL as measured by automatic segmentation of the retina can be affected by edema or atrophy of the retina. In particular, automatic segmentation algorithm errors frequently occur in patients with macular site defects such as macular holes as well as in patients with changes in the shape of the macula due to cystic alterations.

In the present study, the macula was thicker in the affected eyes than in the healthy ones. Furthermore, a comparison of the affected eyes according to the size of the macular hole showed no significant correlations between the size of the macular hole and the thickness of the macula. This is because the macular hole size is mainly determined by tractional force during the development of the macular hole

and because the thickness of the central macula increases as the edge of the macular hole thickens with cystic degeneration [27,28].

The thickness of the GCIPL in affected eyes was 56.1 ± 23.4 µm, which was significantly thinner than the corresponding value in healthy eyes (77.1 ± 12.8 µm). The thicknesses of the GCIPL in groups A and B were 53.7 ± 22.5 and 58.3 ± 23.3 µm, with no significant differences between them. When analyzing the thickness of the GCIPL using the ganglion cell analysis algorithm, oval areas with a horizontal diameter of 1.0 mm and a vertical diameter of 1.2 mm based on the center of the macular area were excluded. Therefore, if the size of the macular hole exceeds 1.2 mm, then the thickness could decrease due to the macular defect; notably, though, the measurement would not be affected by such a defect for a macular hole of ≤400 µm.

However, we found no statistically significant differences between them. The degree of GCIPL thinning was considered to be caused by the boundary of the GCIPL, which was erroneously segmented to be thinner than its actual size because of deformation of the macula, rather than secondary to the influence of the macular hole-induced defect (Fig. 2).

The ICCs for the thicknesses of the central macula, RNFL, and GCIPL of the affected eyes were 0.994, 0.974, and 0.700, respectively. Thus, when measuring the thickness of the central macula and RNFL, the ICC was >0.950 with high repeatability; however, when measuring the GCIPL, the repeatability was low (Table 5). This finding likely resulted from the measurement errors of automatic segmentation caused by deformation of the macula in the affected eyes. Another contributing factor may have been difficulties in the repeated measurement of the same part

caused by instability of fixation secondary to decreased visual acuity accompanied by the macular hole.

There are several limitations in this study. First, because the purpose of the present study was to evaluate the repeatability of OCT measurement by automated analysis without manual adjustment, there could be some measurement error in the central macula, RNFL, and GCIPL thicknesses. Second, it is difficult to apply this method to short eyes (axial length <23.6 mm) or long eyes (axial length >25.5 mm). Further investigations are needed in patients with various axial lengths. Third, we did not evaluate the characteristics of macular hole morphology and the pattern of autosegmentation error. Additional research should be conducted in order to determine the relationship between GCIPL thickness and the pattern of autosegmentation error.

In conclusion, the central macula, peripapillary RNFL, and GCIPL were thicker, similar, and thinner, respectively,
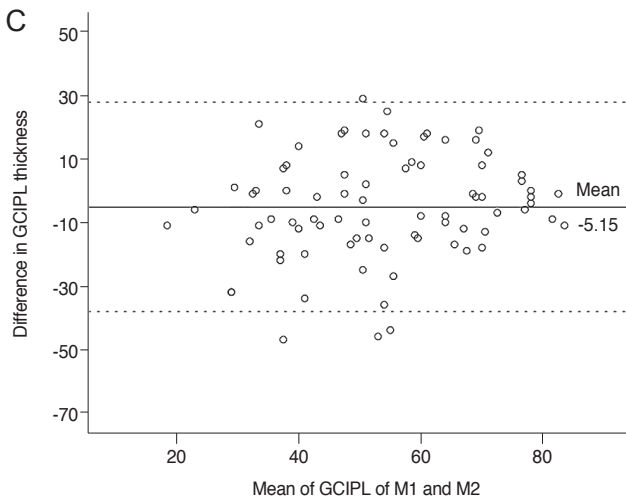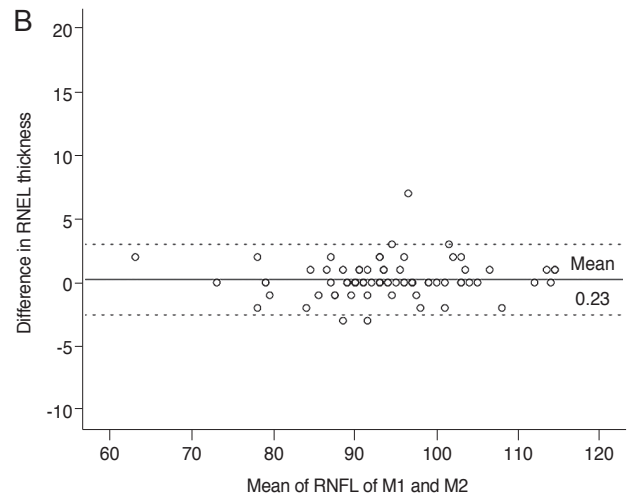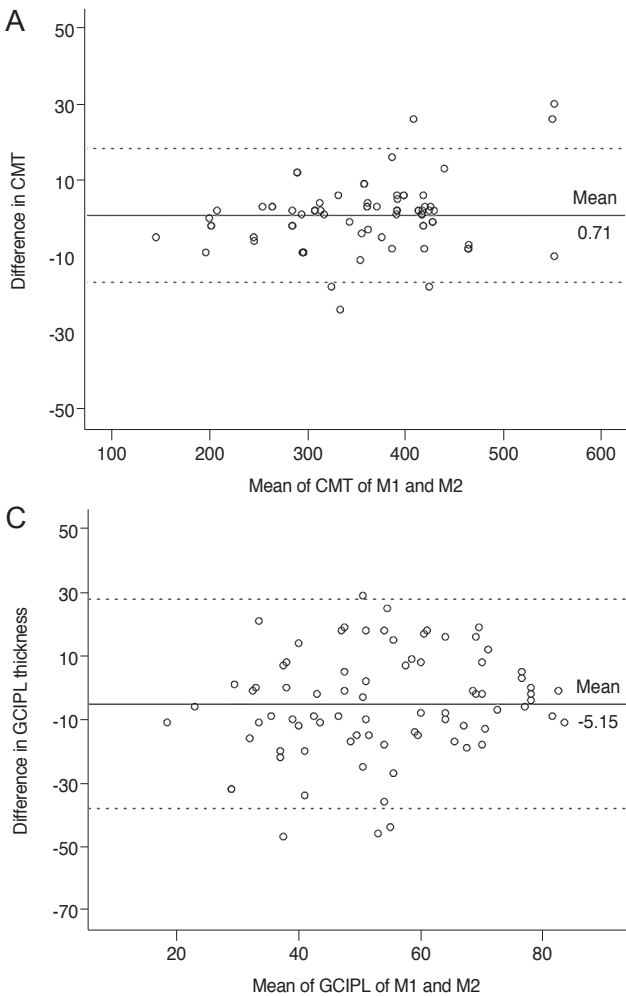
Fig. 3. Blan-Altman plot showing the repeatability of measurements of the central macular thickness (CMT), retinal nerve fiber layer (RNFL), and ganglion cell and inner plexiform layer (GCIPL). The solid line indicates the average mean difference, while the dotted lines lineate the 95% confidence limits of agreement. (A) Bland-Altman plot for the measurements of CMT. The mean difference is 0.71. The 95% limits of agreement are -8.05 to 9.47. (B) Bland-Altman plot for the measurements of RNFL average thickness. The mean difference is 0.24. The 95% limits of agreement are -1.15 to 1.62. (C) Bland-Altman plot for the measurements of GCIPL thickness. The mean difference is -5.15. The 95% limits of agreement are -21.67 to 11.37. M1 = first measurement; M2 = second measurement.

in eyes with macular holes than in the opposite healthy eyes according to SD-OCT evaluation. The repeatability of thickness measurements was lower for the GCIPL than for the central macula and RNFL. Macular contour change with the macular hole results in low repeatability and a tendency to measure thinner GCIPL values using SD-OCT. This may be attributed to unstable fixation with decreased visual acuity and retinal segmentation error due to macular deformation. The impact of changes in the macular shape caused by the presence of macular holes should be taken into consideration when measuring the GCIPL thickness in patients with various eye diseases such as glaucoma and in those with neuro-ophthalmic disorders.

Conflict of Interest

No potential conflict of interest relevant to this article was reported.

References

1. la Cour M, Friis J. Macular holes: classification, epidemiology, natural history and treatment. *Acta Ophthalmol Scand* 2002;80:579-87.
2. Knapp H. About isolated ruptures of the choroid as a result of trauma on the eyeball [Uber isolierte Zerreissungen der Aderhaut in Folge von Traumen auf dem Augapfel]. *Arch Augenheilkd* 1869;1:6-29.
3. Gass JD. Reappraisal of biomicroscopic classification of stages of development of a macular hole. *Am J Ophthalmol* 1995;119:752-9.
4. Gaudric A, Haouchine B, Massin P, et al. Macular hole formation: new data provided by optical coherence tomography. *Arch Ophthalmol* 1999;117:744-51.
5. Hee MR, Puliafito CA, Wong C, et al. Optical coherence tomography of macular holes. *Ophthalmology* 1995;102:748-56.
6. de Sisternes L, Hu J, Rubin DL, Leng T. Visual prognosis of eyes recovering from macular hole surgery through automated quantitative analysis of spectral-domain optical coherence tomography (SD-OCT) scans. *Invest Ophthalmol Vis Sci* 2015;56:4631-43.
7. Xu D, Yuan A, Kaiser PK, et al. A novel segmentation algorithm for volumetric analysis of macular hole boundaries identified with optical coherence tomography. *Invest Ophthalmol Vis Sci* 2013;54:163-9.
8. Krebs I, Hagen S, Brannath W, et al. Repeatability and reproducibility of retinal thickness measurements by optical coherence tomography in age-related macular degeneration. *Ophthalmology* 2010;117:1577-84.
9. Mwanza JC, Budenz DL, Godfrey DG, et al. Diagnostic performance of optical coherence tomography ganglion cell: inner plexiform layer thickness measurements in early glaucoma. *Ophthalmology* 2014;121:849-54.
10. Mwanza JC, Oakley JD, Budenz DL, et al. Macular ganglion cell-inner plexiform layer: automated detection and thickness reproducibility with spectral domain-optical coherence tomography in glaucoma. *Invest Ophthalmol Vis Sci* 2011;52:8323-9.
11. Moon H, Yoon JY, Lim HT, Sung KR. Ganglion cell and inner plexiform layer thickness determined by spectral domain optical coherence tomography in patients with brain lesions. *Br J Ophthalmol* 2015;99:329-35.
12. Francoz M, Fenolland JR, Giraud JM, et al. Reproducibility of macular ganglion cell-inner plexiform layer thickness measurement with cirrus HD-OCT in normal, hypertensive and glaucomatous eyes. *Br J Ophthalmol* 2014;98:322-8.
13. Lee HJ, Kim MS, Jo YJ, Kim JY. Thickness of the macula, retinal nerve fiber layer, and ganglion cell layer in the epiretinal membrane: the repeatability study of optical coherence tomography. *Invest Ophthalmol Vis Sci* 2015;56:4554-9.
14. Hirasawa K, Shoji N, Yoshii Y, Haraguchi S. Determination of axial length requiring adjustment of measured circumpapillary retinal nerve fiber layer thickness for ocular magnification. *PLoS One* 2014;9:e107553.
15. Folio LS, Wollstein G, Ishikawa H, et al. Variation in optical coherence tomography signal quality as an indicator of retinal nerve fibre layer segmentation error. *Br J Ophthalmol* 2012;96:514-8.
16. Cantrill HL. The diabetic retinopathy study and the early treatment diabetic retinopathy study. *Int Ophthalmol Clin* 1984;24:13-29.
17. Muller R, Buttner P. A critical discussion of intraclass correlation coefficients. *Stat Med* 1994;13:2465-76.
18. Bland JM, Altman DG. Statistical methods for assessing agreement between two methods of clinical measurement. *Lancet* 1986;1:307-10.
19. Barak Y, Ihnen MA, Schaal S. Spectral domain optical coherence tomography in the diagnosis and management of vitreoretinal interface pathologies. *J Ophthalmol*

2012;2012:876472.

20. Takahashi H, Kishi S. Tomographic features of a lamellar macular hole formation and a lamellar hole that progressed to a full-thickness macular hole. *Am J Ophthalmol* 2000;130:677-9.

21. Liu X, Shen M, Huang S, et al. Repeatability and reproducibility of eight macular intra-retinal layer thicknesses determined by an automated segmentation algorithm using two SD-OCT instruments. *PLoS One* 2014;9:e87996.

22. Budenz DL, Fredette MJ, Feuer WJ, Anderson DR. Reproducibility of peripapillary retinal nerve fiber thickness measurements with stratus OCT in glaucomatous eyes. *Ophthalmology* 2008;115:661-6.

23. Pinilla I, Garcia-Martin E, Fernandez-Larripa S, et al. Reproducibility and repeatability of Cirrus and Spectralis Fourier-domain optical coherence tomography of healthy and epiretinal membrane eyes. *Retina* 2013;33:1448-55.

24. Park KA, Park DY, Oh SY. Analysis of spectral-domain optical coherence tomography measurements in amblyopia: a pilot study. *Br J Ophthalmol* 2011;95:1700-6.

25. Kim JJ, Im JC, Shin JP, et al. One-year follow-up of macular ganglion cell layer and peripapillary retinal nerve fibre layer thickness changes after panretinal photocoagulation. *Br J Ophthalmol* 2014;98:213-7.

26. Garas A, Vargha P, Hollo G. Reproducibility of retinal nerve fiber layer and macular thickness measurement with the RTVue-100 optical coherence tomograph. *Ophthalmology* 2010;117:738-46.

27. Ullrich S, Haritoglou C, Gass C, et al. Macular hole size as a prognostic factor in macular hole surgery. *Br J Ophthalmol* 2002;86:390-3.

28. Kusuhara S, Teraoka Escano MF, Fujii S, et al. Prediction of postoperative visual outcome based on hole configuration by optical coherence tomography in eyes with idiopathic macular holes. *Am J Ophthalmol* 2004;138:709-16.